Experimental investigation on pulse-contrast degradation caused by surface reflection in optical parametric chirped-pulse amplification

Xinliang Wang (王新亮)[1,2,3], Xiaoming Lu (陆效明)[2], Xiaoyang Guo (郭晓杨)[4], Rongjie Xu (许荣杰)[2], and Yuxin Leng (冷雨欣)[2,3,*]

[1]*School of Physics Science and Engineering, Tongji University, Shanghai 200092, China*
[2]*Shanghai Institute of Optics and Fine Mechanics, Chinese Academy of Sciences, Shanghai 201800, China*
[3]*University of Chinese Academy of Sciences, Beijing 100049, China*
[4]*Osaka University, Osaka 565-0871, Japan*
**Corresponding author: lengyuxin@mail.siom.ac.cn*

Received January 3, 2018; accepted April 3, 2018; posted online April 27, 2018

In this Letter, we experimentally explore the pulse-contrast degradation caused by surface reflection in optical parameter chirped-pulse amplification. Different pump-to-signal conversion efficiencies and post-pulses with different intensities are obtained by changing the seed-pulse or pump-pulse energy and inserting etalons with different reflection coefficients, respectively. The contrast measurements show that the generated first pre-pulse intensity is proportional to the product of the surface reflection intensity ratio and the square of the pump-to-signal conversion efficiency.

OCIS codes: 190.4410, 320.7110.
doi: 10.3788/COL201816.053201.

The development of chirped-pulse amplification (CPA)[1] and optical parametric CPA (OPCPA)[2–4] technology provides an extreme tool to study laser–matter interactions in the relativistic regimes with on-target intensity exceeding 10^{22} W/cm^2. So far, several 5 PW level laser systems have been built among the world based on either CPA[5,6] or OPCPA[4] technology. Compared with CPA, OPCPA has many advantages, such as high single-pass gain, broadband gain bandwidth, and low thermal loading effects. These features make it a very attractive technique to generate ultra-short laser pulses in multi-petawatt (PW) laser systems.

During the amplification of laser pulses, the pulse contrast may be degraded significantly, which is caused by isolated pre-pulses or by a slowly varying pedestal after pulse recompression. Since the intensity of noise above the ionization threshold of the solid target could ionize the target before the main pulse arrives, which would radically modify the laser–plasma interaction processes[7], the corresponding experiments require high contrast[8]. Basically, the long-time-range pedestal is usually caused by the amplified spontaneous emission (in CPA systems)[9] or parametric fluorescence (in OPCPA systems)[10] generated in the amplified process, which could be overcome by injecting a high-energy, high-contrast seed, or the high-frequency noise pedestal generated in the stretcher, which could be improved by avoiding the far-field high-frequency noise[11]. The pre-pulses are usually transformed from the post-pulses caused by surface reflection of the optical components in laser systems. Generally, there exist several generation mechanisms about the pre-pulses. In some amplifiers, such as a regenerative amplifier or a double-pass amplifier, some post-pulses may experience different paths with the main pulse, therefore, they go ahead of the main pulse and become pre-pulses[12]. This case can be avoided by carefully designing the amplifier or using wedged optical components. Didenko *et al.* have reported that the post-pulses can also lead to pre-pulses under the nonlinear effect in the amplification process[13]. Recently, Qian *et al.* have theoretically studied a novel mechanism of surface-reflection-initiated pulse-contrast degradation in an OPCPA system by an analytical approach together with numerical simulations[14]. According to their analysis, the pre-pulses are initiated from the surface-reflection-induced modulation of the seed spectrum and occur as a consequence of high-order distortion of such modulated spectrum. The intensity of the first pre-pulse increases quadratically with the initial temporal modulation depth of the stretched signal pulse, as well as the conversion efficiency prior to substantial pump depletion. However, they have not presented the experimental results to support it.

In this Letter, we perform the experimental investigations, which verify that the post-pulses may lead to the pre-pulses in an OPCPA system. Our experiments are carried out in a high-contrast 1053 nm laser system. To investigate the relation between the post- and generated pre-pulse, etalons with different reflection ratios are used to generate post-pulses with different intensities. Besides, the pump and seed intensities are also changed during the experiment to vary the pump-to-signal conversion efficiency. The experimental results reveal that the intensity of the generated first pre-pulse is proportional to the product of the intensity ratio of the surface reflection and the

square of the pump-to-signal conversion efficiency when the OPCPA system is running in the non-saturation region. Therefore, in the design of a high-contrast OPCPA system, the post-pulses should be carefully avoided.

Our experiment is carried out in the high-contrast laser system[11,15]. Here, only the OPCPA stages are used, and the Nd:glass amplifiers are bypassed (Fig. 1). The 1053 nm high-contrast seed pulse generated in the 800 nm femtosecond (fs) pulse pumped optical parametric amplifier (OPA) is stretched to about 1.1 ns in a Martinez two-lens stretcher. The 60 μJ stretched pulse is then amplified in the two OPCPA stages. At the 160 mJ pump energy, the amplified energy is measured to be 10.5 mJ. After the amplified pulse is compressed in the two-grating compressor, a scanning third-order autocorrelator (Sequoia-1000, Amplitude Technologies) is used to measure the contrast. The amplified spectrum (see the inset in Fig. 2) shows that the OPCPA amplifier is operating at a non-saturated state, which suppresses the generation of the parametric fluorescence. In the following experiment, the energy of the pump laser is controlled lower than 180 mJ to avoid damaging the windows of the vacuum tube used for image-relaying the pump laser.

Weak post-pulses after the seed pulse are created by inserting a 5 mm thick fused silica etalon without coating (E1) into the beam perpendicular to its axis. The etalon is inserted between the pulse clean device (OPA) and pulse stretcher (see Fig. 1). The measured intensities of the first and second post-pulses [Fig. 3(a)] at 48.4 and 96.8 ps are close to the levels deduced by the Fresnel reflection: 1.16×10^{-3} and 1.35×10^{-6}, respectively. When the OPA is running in the saturation region, the reconversion results in the post-pulses experiencing higher gain than the main pulse. Hence, the measured intensities of the first and second post-pulses should be higher than the levels deduced by the Fresnel reflection, which further proves the OPCPA system operating in the non-saturation region. In the contrast scanning measurement, at the mirror position of a real post-pulse, there may exist a false pre-pulse, which is caused by interaction of the second harmonic of the post-pulse and the fundamental of the main peak. In this case, $I_{\mathrm{pre-pulse}} = I_0 \cdot I^2_{\mathrm{post-pulse}}$. Therefore, the measured first pre-pulse (2.13×10^{-4}) at the delay of −48.4 ps is obviously not a ghost pulse. Meanwhile, the contrast scanning without an etalon inserted shows that there is no pre-pulse [blue line in Fig. 3(a)]. Therefore, we can conclude that the first pre-pulse is generated by the interaction of OPCPA and the first post-pulse induced by the etalon.

In the following, we experimentally study the relationship between the intensity of the first pre-pulse and the main pulse by changing two parameters η and r, which stand for the pump-to-signal conversion efficiency and

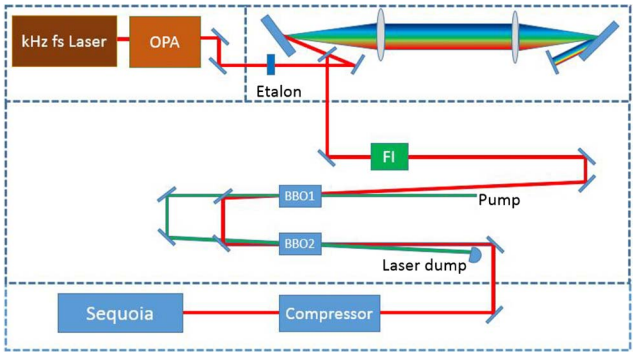

Fig. 1. Schematic of experimental setup.

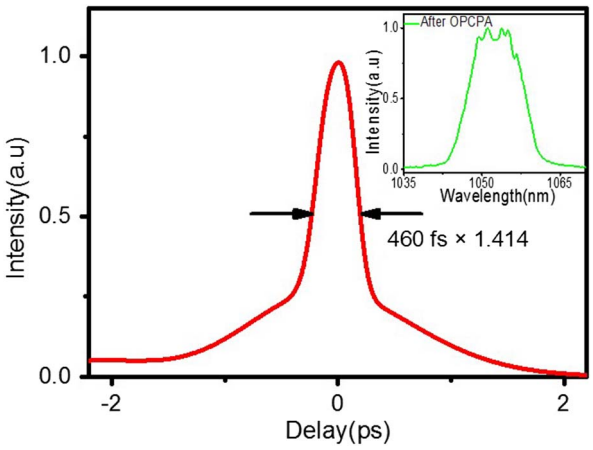

Fig. 2. Autocorrelation trace of the amplified pulse. The inset is the spectrum after the two OPCPA stages.

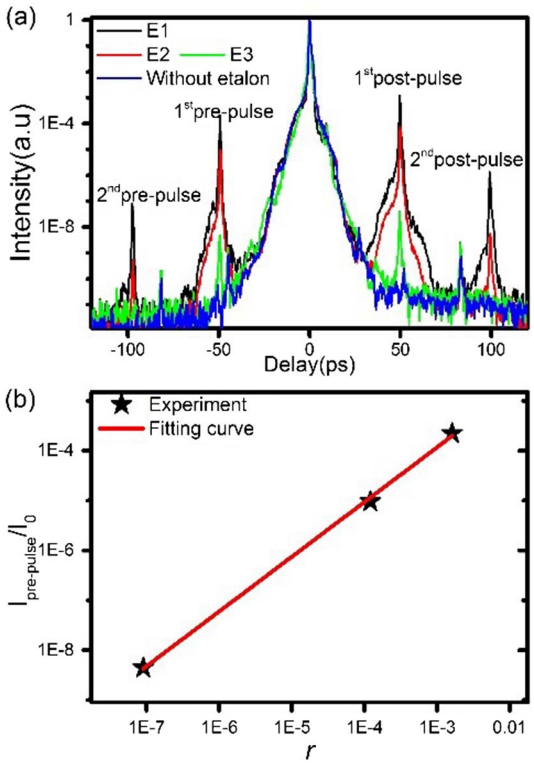

Fig. 3. (a) Contrast scanning results of compressed pulses with different etalons (E1, black line; E2, red line; E3, green line) and without an etalon (blue line). (b) Measured intensities of the first pre-pulses varying with the surface reflection ratio r.

the ratio of the surface reflection, respectively. The surface reflection ratio r is proportional to the square of the sinusoidal modulation depth of the seed spectrum induced by the interference between the first post-pulse and the main pulse. The pump-to-signal conversion efficiency η stands for the depletion of the pump light.

To analyze the relationship between the intensity of the first pre-pulse and the surface reflection ratio r, other two etalons with different coatings are also used in the experiment: E2 with a single antireflection (AR) coating of about 0.30%, and E3 with double AR coatings of about 0.03%. In the contrast measurement, the pump (160 mJ) and seed (60 μJ) are fixed. Figure 3(a) shows the measured intensities of the first pre-pulses for different etalons, which have values of 2.13×10^{-4}, 9.63×10^{-6}, and 4.43×10^{-9}, respectively. The results show a direct proportion between $I_{\mathrm{pre-pulse}}/I_0$ and r, as shown in Fig. 3(b) by the fitting curve. Besides, the second pre-pulses are observed in the experiment at the delay of −96.8 ps for E1 and E2 [see Fig. 3(a)], which have the intensities of 8.23×10^{-8} and 5.43×10^{-10}, respectively. The measured second pre-pulse actually corresponds to the first pre-pulse caused by the second post-pulse, because the intensity of the second pre-pulse caused by the first post-pulse should be smaller than the square of that of the first pre-pulse, according to the analysis in Ref. [14]. Additionally, thanks to the small reflection ratio of E3, the corresponding second pre-pulse exceeds the dynamic range of the instrument and, hence, cannot be measured.

During the OPCPA progress, the pump-to-signal conversion efficiency is decided by both the energy of the pump and seed pulse. Next, we use E1 to generate a post-pulse with a constant initial post-pulse intensity ratio r while changing the pump and seed energy. Through this, we further investigate the relationship between the intensity of the first pre-pulse and the pump-to-signal conversion efficiency η. The seed energy is changed by inserting a neutral density filter (NE06 A, Thorlabs) before the OPCPA system, which has a 23.6% energy transmission ratio at 1053 nm. Meanwhile, we can also change the pump energy. With the neutral density filter inserted, 2.80%, 3.47%, and 4.22% pump-to-signal efficiencies are obtained when the energy of the pump laser increases from 160 and 170 mJ to 180 mJ. Another intensity data is measured with 6.56% conversion efficiency when the pump energy is 160 mJ without the neutral density filter. With η increasing from 2.80% to 6.56%, the relative intensity of the first pre-pulse increases from 3.53×10^{-5} and 6.34×10^{-5} to 9.96×10^{-5} and then to 2.13×10^{-4}, showing a linear proportion between $I_{\mathrm{pre-pulse}}/I_0$ and η^2 (see Fig. 4). A higher η stands for higher nonlinear coupling strength between the modulated signal and the pump light, which results in more serious pulse-contrast degradation.

In the experiments discussed above, either the pump-to-signal conversion efficiency η or the intensity ratio r is considered separately. Here, the relationship of the intensity of the pre-pulse with the pump-to-signal conversion efficiency η and intensity ratio r is comprehensively considered by implementing eight scenarios with the parameters listed in Table 1. The intensity ratio r is controlled by using etalons with different coatings. Meanwhile, the pump-to-signal conversion efficiency η is adjusted by manipulating the pump energy, the seed energy, and the thickness of the beta-barium borate (BBO) crystal. When adjusting the parameter of η, the energy of the seed pulse is adjusted by whether the neutral density filter is used or not, while the length of the crystal is controlled by using two BBO crystals or only the first BBO crystal in the OPCPA amplifier. With the detailed experimental parameters listed in Table 1, Fig. 5 gives the experiment results and the fitting curve. Obviously, the intensities of

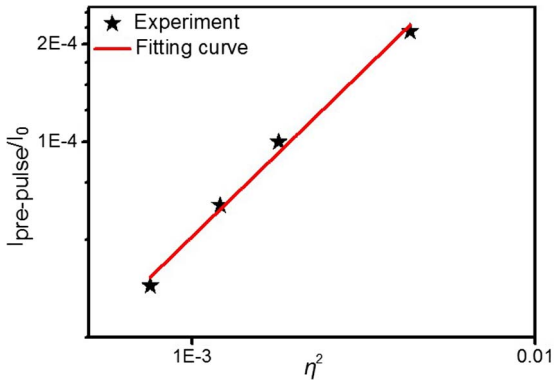

Fig. 4. Measured intensities of the first pre-pulses with different pump-to-signal conversion efficiencies.

Table 1. Parameters in OPCPA Amplifiers and Measured Intensities of the First Pre-pulses

Number	1	2	3	4	5	6	7	8
Etalon	E1	E1	E1	E1	E2	E2	E2	E3
Attenuation	NE06A	NE06A	NE06A	None*	None	None	NE06A	None
Crystal	Both	Both	Both	Both	Both	First	First	Both
Pump/mJ	160	170	180	160	160	160	160	160
Signal/mJ	4.48	5.9	7.6	10.5	10.5	4.5	1.9	10.5
Contrast	3.53×10^{-5}	6.34×10^{-5}	9.96×10^{-5}	2.13×10^{-4}	9.63×10^{-6}	3.02×10^{-6}	1.52×10^{-7}	4.43×10^{-9}

*Without the neutral density filter (NEO6A) inserted.

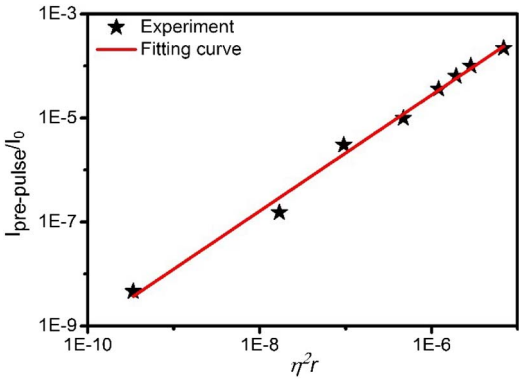

Fig. 5. Measured intensities of the first pre-pulses by using parameters listed in Table 1.

the pre-pulses are proportional to the product of reflection ratio r and the square of the pump-to-signal conversion ratio η^2. The experimental values compare well quantitatively with values predicted as the following analytic equation[14]:

$$\frac{I_{\mathrm{pre-pulse}}}{I_0} \propto \eta^2 r, \tag{1}$$

where $I_{\mathrm{pre-pulse}}$ and I_0 are the intensity of the first-order pre-pulse and the main pulse, respectively. Surface reflection is a common phenomenon in a large laser system; hence, the impact of surface-reflections-induced contrast degradation cannot be ignored. Therefore, measures, such as coating and wedging the transmissive optical elements, should be taken to minimize the surface reflectivity.

In conclusion, we perform experiments to demonstrate that pre-pulses can be generated in an OPCPA system due to the existence of the surface reflection. The experimental results reveal that the intensity of the first pre-pulse is well confirmed to the proportional relationship with the product of the intensity ratio of the surface reflection and the square of the pump-to-signal conversion efficiency. The verified new pulse contrast degradation mechanism reminds us that the impact of surface-reflections-induced contrast degradation should be carefully considered when a high-contrast OPCPA system is designed. To obtain a further understanding of the pre-pulse generation in OPCPA systems, more work should be carried out in the future, such as the first pre-pulse generation in the case of OPCPA saturation operation.

This work was supported by the Strategic Priority Research Program of the Chinese Academy of Sciences (No. XDB1603), the International S&T Cooperation Program of China (No. 2016YFE0119300), and the National Natural Science Foundation of China (NSFC) (Nos. 61521093 and 61505234).

References

1. D. Strickland and G. Mourou, Opt. Commun. **55**, 447 (1985).
2. C. Dorrer, I. A. Begishev, A. V. Okishev, and J. D. Zuegel, Opt. Lett. **32**, 2143 (2007).
3. D. N. Papadopoulos, P. Ramirez, K. Genevrier, L. Ranc, N. Lebas, A. Pellegrina, C. Le Blanc, P. Monot, L. Martin, J. P. Zou, F. Mathieu, P. Audebert, P. Georges, and F. Druon, Opt. Lett. **42**, 3530 (2017).
4. X. Zeng, K. Zhou, Y. Zuo, Q. Zhu, J. Su, X. Wang, X. Wang, X. Huang, X. Jiang, D. Jiang, Y. Guo, N. Xie, S. Zhou, Z. Wu, J. Mu, H. Peng, and F. Jing, Opt. Lett. **42**, 2014 (2017).
5. Z. Gan, L. Yu, S. Li, C. Wang, X. Liang, Y. Liu, W. Li, Z. Guo, Z. Fan, X. Yuan, L. Xu, Z. Liu, Y. Xu, J. Lu, H. Lu, D. Yin, Y. Leng, R. Li, and Z. Xu, Opt. Express **25**, 5169 (2017).
6. J. H. Sung, H. W. Lee, J. Y. Yoo, J. W. Yoon, C. W. Lee, J. M. Yang, Y. J. Son, Y. H. Jang, S. K. Lee, and C. H. Nam, Opt. Lett. **42**, 2058 (2017).
7. D. Neely, P. Foster, A. Robinson, F. Lindau, O. Lundh, A. Persson, C. G. Wahlström, and P. McKenna, Appl. Phys. Lett. **89**, 021502 (2006).
8. J. Gao, F. Liu, X. Ge, Y. Deng, G. Zhang, Y. Fang, W. Wei, S. Yang, X. Yuan, M. Chen, Z. Sheng, and J. Zhang, Chin. Opt. Lett. **15**, 081902 (2017).
9. J. Itatani, J. Faure, M. Nantel, G. Mourou, and S. Watanabe, Opt. Commun. **148**, 70 (1998).
10. K. Kondo, H. Maeda, Y. Hama, S. Morita, A. Zoubir, R. Kodama, K. A. Tanaka, Y. Kitagawa, and Y. Izawa, J. Opt. Soc. Am. B **23**, 231 (2006).
11. X. Lu, X. Wang, Y. Leng, X. Guo, Y. Li, Y. Peng, R. Xu, Y. Xu, and X. Qi, IEEE J. Sel. Top. Quantum Electron. **24**, 1 (2018).
12. S. Keppler, R. Bödefeld, M. Hornung, A. Sävert, J. Hein, and M. C. Kaluza, Appl. Phys. B **104**, 11 (2011).
13. N. V. Didenko, A. V. Konyashchenko, A. P. Lutsenko, and S. Y. Tenyakov, Opt. Express **16**, 3178 (2008).
14. J. Wang, P. Yuan, J. Ma, Y. Wang, G. Xie, and L. Qian, Opt. Express **21**, 15580 (2013).
15. X. Lu, Y. Peng, Y. Li, X. Guo, Y. Leng, Z. Sui, Y. Xu, and X. Wang, Chin. Opt. Lett. **14**, 023201 (2016).